The SPEAR Science Payload

Eric J. Korpela[a], Jerry Edelstein[a], Peter Berg[a], Mark Bowen[a],
Ray Chung[a], Michael Feuerstein[a], Wonyong Han[b], Jeffrey S. Hull[a], Ho Jin[b],
Daehee Lee[c], Kyoung Wook Min[c], Uk-Won Nam[b], Kaori Nishikida[a], Jin Geun Rhee[b],
Kwangsun Ryu[c], Kwang-Il Seon[b], Barry Y. Welsh[a], In-Soo Yuk[b]

[a]Space Science Laboratory
University of California,
Berkeley, CA 94720-7450

[b]Korea Astronomy Observatory
61-1, Hwaam-dong, Yusong-gu
Taejon 305-348, Korea

[c]Satellite Technology Research Center
Korea Advanced Institute of Science and Technology
373-1 Kusong-dong, Yusong-gu
Taejon 305-701, Korea

ABSTRACT

The SPEAR micro-satellite payload consists of dual imaging spectrographs optimized for detection of the faint, diffuse FUV (900-1750 Å) radiation emitted from interstellar gas. The instrument provides spectral resolution, R~750, and long slit imaging of <10′ over a large (8°×5′) field of view. We enhance the sensitivity by using shutters and filters for removal of background noise. Each spectrograph channel uses identically figured optics: a parabolic-cylinder entrance mirror and a constant-ruled ellipsoidal grating. Two microchannel plate photon-counting detectors share a single delay-line encoding system. A payload electronics system conditions data and controls the instrument. We will describe the design and predicted performance of the SPEAR instrument system and its elements.

Keywords: Diffuse ultraviolet spectroscopy, ultraviolet detectors, interstellar medium, SPEAR, microchannel plate detectors.

1. INTRODUCTION

The SPEAR (Spectroscopy of Plasma Evolution from Astrophysical Radiation) mission is scheduled for launch in the second half of 2003 aboard the Korean science satellite KAISTSAT-4. It will conduct a sensitive all-sky survey of diffuse far ultraviolet (900-1750 Å) emission from interstellar and intergalactic matter. [Edelstein et al., 2002] The primary science objectives of this mission include mapping the flow of mass and energy through the interstellar medium (ISM), mapping the global distribution of the multiphase interstellar medium, and testing contentious models for the origin of the hot interstellar plasma. Secondary goals include a sensitive survey of Galactic diffuse H_2 fluorescence, investigation of interstellar dust properties and distribution, and a search for intergalactic intermediate temperature plasmas.

Correspondence: Email: *korpela@ssl.berkeley.edu*; Telephone: *(510) 643-6538*;
URL: *http://setiathome.ssl.berkeley.edu/~korpela*

We have chosen dual imaging spectrographs, optimized for faint diffuse radiation to achieve our science objectives. SPEAR's Short λ channel (Sλ) covers λλ 900 - 1175 Å and its Long λ channel (Lλ) covers λλ 1335 - 1750 Å. The channels include the important O VI λλ 1035 Å and CIV λλ 1550 Å multiplets. The field of view is 4°x5' for Sλ and 8°x5' for Lλ with 5-10' imaging resolution along the slit. Extreme care has been taken to mitigate the airglow, stellar and instrumental noise sources that often plague FUV measurements.

SPEAR's sensitivity is unprecedented: in pointed observations of 12 ksec (i.e., 24 hours of operations) SPEAR will achieve a 3-σ measurement sensitivity of 260 photon s^{-1} cm^{-2} sr^{-1} (LU) and 170 LU for the O VI and C IV doublets, respectively. In astronomical units, these intensities correspond to ~ 0.0001 EM (cm^{-6} pc), or in physical units $3x10^{-9}$ erg s^{-1} cm^{-2} sr^{-1}. In comparison to previous measurements of interstellar FUV emission, SPEAR would detect the FUSE [Dixon et al., 2001, Shelton et al., 2001] and UVX [Martin & Bowyer, 1990] measured intensities of 2,300 LU of O VI λλ 1035 Å and 5,000 LU of C IV λλ 1550 Å with a S/N of 36 and 90, respectively. In similar fashion, for the average sky-map exposure in 4,500 bins of 3°x3°, the FUSE and UVX intensities would be measured with a S/N of 7 and 23.

Our rationale for selecting simple slit-spectroscopy for mapping the sky is based upon 1. our flight experience with EURD using this method for faint diffuse measurements [Bowyer et al. 1999, Edelstein et al. 2001, Lopez-Moreno et al. 2001]; 2. the desirability of measuring a broad bandpass to prospect for ISM FUV diagnostics; 3. avoiding the use of high diffraction orders (unreliable efficiencies & scattering, low order contamination); 4. avoiding the use of fluorescent crystal fluoride optics in full view of the detector; 5. avoiding moisture sensitive coatings (e.g. unprotected LiF); and 6. use of simple "pushbroom" imaging spectroscopy which is relatively insensitive to background variations, and is relatively simple to analyze.

2. INSTRUMENT SCIENCE REQUIREMENTS

Prime instrument science requirements regard bandpass, spectral resolution, sensitivity, field of view (FOV), and imaging resolution. (See Table 1 for a summary). Key secondary requirements include noise-source suppression.

Our dual bandpass scheme has been chosen to include a very wide range of ionic species while avoiding intense geocoronal line contamination. Consequently, plasma equilibrium, abundance and photoionization effects can be independently measured. SPEAR's broadband coverage is essential because of the divergent range of model equilibrium state predictions and because SXR data [McCammon et al., 1999] are indicative of non-equilibrium or depleted conditions. Coincidentally, SPEAR's bandpass is also ideally suited for measuring H2 fluorescence.

SPEAR must distinguish diagnostic lines from each other and from bright airglow lines. Simulations show that the most critical spectral resolution requirement is to isolate the important O VI 1032 Å line from intense Ly β 1027 Å airglow. The instrumental line profile and O VI and Ly β intensities determine the quality of isolation.

We performed a Monte-Carlo analysis of OVI measurement significance as a function of OVI intensity and raytraced spectral profile. [Seon et al. 2000] We found that Δλ = 1.7 Å HEW is needed to achieve our sensitivity goals.

Item	Requirement	Performance
Sensitivity (3σ)		
Sky Survey (3°x3°)	2500 LU OVI 5000 LU CIV	980 LU 650 LU
Pointed Obs. (1 orbit)	1500 LU	400-700LU
Imaging (along slit)	10'	<7.5'
Spectral Resolution	1.7 Å OVI 2.5 Å CIV	1.4 Å 2.2 Å
Alignment to S/C bus	3'	1.2'
Pointing Knowledge	5'	3.2'
Pointing Accuracy	20'	15'
Power	25 W	22 W
Mass	22 kg	20.5 kg
Temperature Range**	0–25° C	-15–40° C
Maximum Data Rate	500 c/s	5000 c/s
Payload Science Memory	3 kbyte	300 kbyte
Normal Operations	195 kbyte	300 kbyte
Contingency Ops.		
Output Data Rate		
Normal Operations	16 kbps	200 kbps
Contingency Ops.	3 kbps	4 kbps

Table 1: Summary of Instrument Requirements

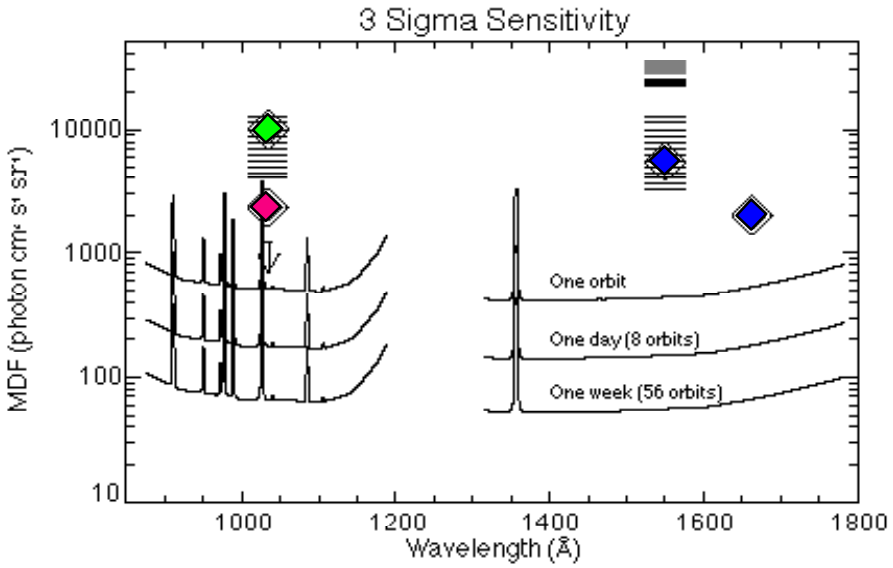

Figure 1: SPEAR sensitivity for 1 orbit, 1 day and 1 week pointed observations. The diamonds show values measured by FUSE, HUT and UVX. The hatched regions show typical values predicted by galactic fountain models

SPEAR's raytraced resolution over its full slit height is 1.4 Å HEW at 1032 Å. Raytracing tolerance studies show that our thermal and alignment tolerances do not violate the >20% spectral performance margin. In the Long λ channel, stellar continuum limits sensitivity. We chose a 2.5 Å HEW resolution requirement for the separation of spectral lines and limitation of continuum noise. Raytrace analyses over the full slit shows a 2.2 Å HEW resolution over most of the band.

SPEAR's sensitivity must test predictions of global models of the ISM which range from a few 100 LU, for emission from the Local Bubble, to 10,000's LU for coronal cooling and supernova shocks. These sensitivities must be achieved in 24 mission hour pointings to allow observation of the desired hundreds of targets in a year. Sensitivity for the sky-map must yield angular sky-bin samples of sufficient quantity (thousands) to obtain robust correlation with other tracers of hot and cool gas. We feel that a conservative approach is for our instrument's 3-σ measurement error to surpass previously observed values of 2-5 k LU by an order of magnitude. (See Fig 1)

The 10' image mapping requirement is desired for small-feature correlations with similar angular scale maps in other wave-bands and for observations of extragalactic sources, SNR shocks and H2 nebulae features. Small scale correlation of FUV emission with neutral and molecular ISM tracers will be of great value to understanding IS morphology. The science objective, to measure diffuse ISM properties, is very tolerant to the imaging performance because the diffuse ISM itself is a large target and because the loss of observing time due to bright star contamination represents a small fraction of the total (<15 - 20%) even with imaging performance degraded by factors of several. The instrument's optical resolution is designed to deliver 2 - 7' imaging, depending on the imaging angle. The K-4 pointing knowledge requirement of 6' is combined in quadrature to yield the <10' expected sky-map performance.

The sky exposure per map-pixel is a function of the ecliptic latitude. Our 10' mapping pixels may be integrated over features as dictated by ISM morphology or in fixed size or exposure bins. Fig. 2 shows the relationship of sensitivity versus integrated solid angle compared with the intensity of astronomical objects. Sensitivity for features smaller than the slit length is determined by the effective exposure per sky-pixel. For small sky pixels and exposures, the sensitivity becomes photon limited. Bright features such as SNR structures, with measured intensities of 10,000's of LU, can readily be measured both in the Survey and in pointings. A 10' feature has a 1200-1800 LU MMF for a 24-hour pointing.

Each SPEAR spectral resolution element independently measures continuum radiation. Thus, SPEAR's continuum 3σ MMF for a 24 hour observation over a 50 Å bandpass (20 / 30 spectral bins in the Lλ / Sλ channel), is 40-50 LU. SPEAR's continuum sensitivity will easily detect the 100's to 1000's LU/ Å of dust-scattered continuum observed with Voyager.

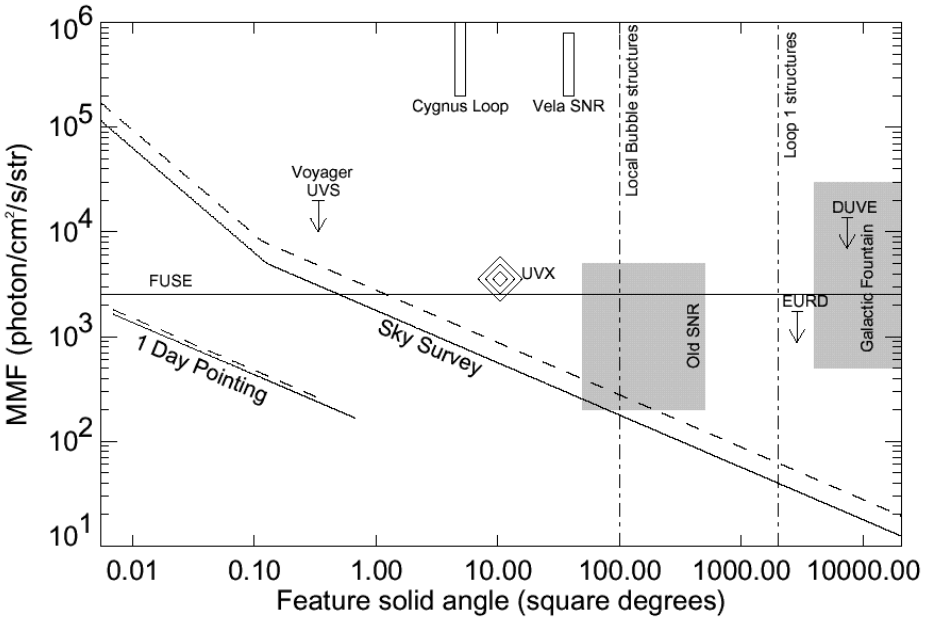

Figure 2: Sensitivity of SPEAR to features of different angular size. Model predictions are shown as shaded areas. Existing measurements or limits by EURD, DUVE, UVS,

Because SPEAR measurements are background limited for all but very short exposures, the sensitivity scales as the square root of the background rate and throughput. Consequently, sensitivity performance has significant tolerance to throughput losses and to airglow, continuum, and similar noise contributors.

Several features of the design have been implemented as a means of fitting into the mass, power, and financial budgets of this small program. 1) The design, especially of the electronics, is largely based upon our previous flight systems, reducing the engineering effort which would be required to implement a new low-heritage design. 2) Use of small format round microchannel plates reduces cost (over large format rectangular plates) while improving instrument performance. 3) Use of a single detector anode for both optical systems reduces the power budget and mass of the detector electronics. 4) The Sλ and Lλ optical elements share a common surface figure which reduces fabrication costs. 5) Modular mechanical design allows independent subsystem development and test until late in the integration flow.

3. OPTICAL DESIGN

SPEAR uses a proven grating-mount method for large-grasp imaging spectroscopy. Each spectrograph channel consists of a collecting mirror, slit, filter, grating and detector. For simplicity, each channel uses identically-figured 5x8 cm optics, a cylindrical telescope mirror and an elliptical figure, constant line-space grating in the same geometrical mount that shares the same slit and detector focal plane. (See Fig. 3) This cylindrical source method provides twice the grasp and field of standard spectrographs, even with fast (f/2.2) figure optics. The imaging performance allows for a large field with imaging resolution (arcminute scales) similar to other important all-sky surveys of interstellar matter (see Fig. 4).

The SPEAR design is derived directly from the EURD instruments [Edelstein, Dixon, & Korpela 1999]. Subassemblies are mounted in a box structure that will be integrated into the spacecraft structure (See Fig. 5). Thermal, structural and tolerance analyses showed that a 6061 Al structure would suffice. The dual bandpass allows for independent, optimized choices for the reflective coatings (BC/MgF2) and detector photocathode (RbBr/CsI) for the Short and Long channels. (BC is chosen over SiC because it is impervious to attack by atomic oxygen.)

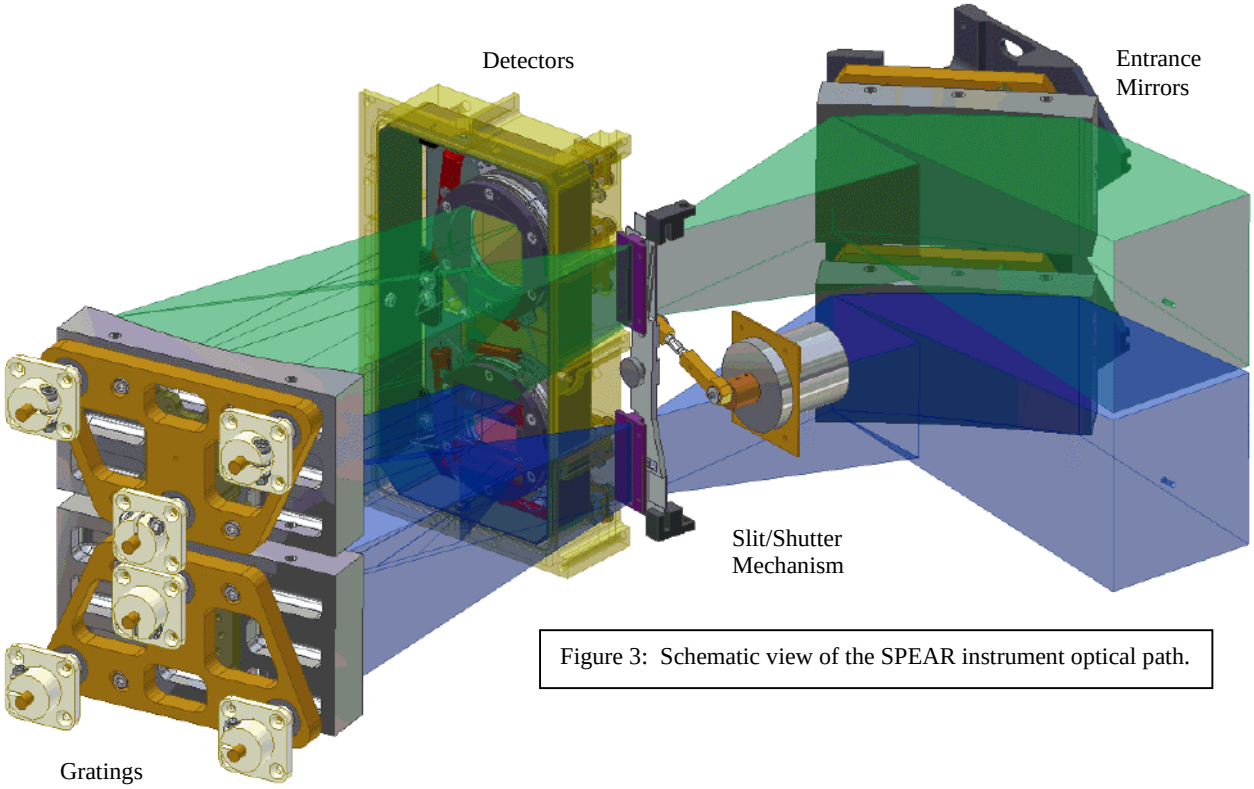

Figure 3: Schematic view of the SPEAR instrument optical path.

The collecting mirrors were made using commercial grinding and polishing techniques and the UV filters, coatings and photocathodes are similar to those used on several previous SSL missions. The diffraction grating uses a blazed profile produced by chemically etching a holographically formed pattern into glass. Test gratings produced by this method confirm 65% diffraction efficiency and low scattering ($1x10^{-5}$/'). Parabolic cylinder mirrors have been fabricated by CVI Korea. Flight diffraction gratings have been manufactured by Zeiss, and are scheduled for delivery between the time of this writing and the time of publication.

We have performed an optical tolerance analysis to determine the required precision and range of motion of the optics and detector mounts. The analysis determined the range by considering the effects of motion in each of the possible adjustments and the potential of offsetting these effects with translation or rotation of other mounts. [Ryu et al. 2000]. More details of the SPEAR optical design are presented in Ryu et al. [2002].

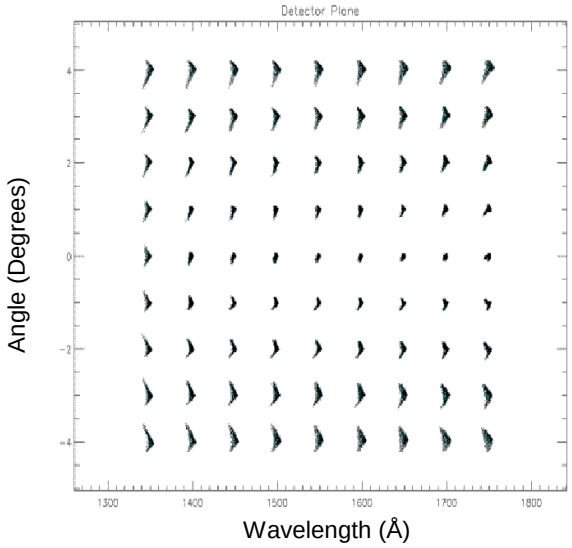

Figure 4: Raytracing was used to model instrument resolution. The design provides 5'8 arcminute imaging and 1.4-2 Å spectral resolution over an 8 degree field of view.

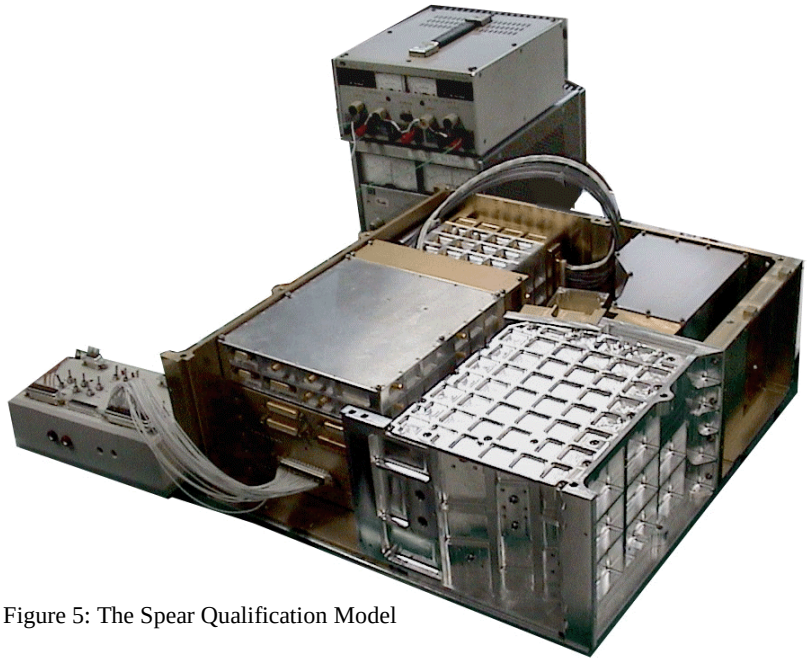

Figure 5: The Spear Qualification Model

3.1 Noise Reduction

We have taken great care to reduce noise from airglow lines, stars, scattered continuum starlight, detector and ion background and optics fluorescence. Instrumentally scattered Ly α is the dominant noise source in the Short channel and requires special attention for accurate removal from the data. We have included a filter and shutter that allows for statistically unbiased removal of instrumentally scattered light and detector background, an important task in the Short bandpass (The shutter exposure loss was included in our sensitivity calculations.)

For the Sλ channel, Ly α noise will be measured simultaneously with the signal because it can vary markedly on hour time-scales. We provide independent and simultaneous measurement of Ly α noise by measuring the sky at the top and bottom quarter of the 8° field of view through a MgF_2 filter at the detector.

The Long λ channel views the sky through a CaF_2 filter, which has the property of blocking wavelengths less than 1230 Å. We analyzed 1) the effect of our orbit radiation environment on the florescence rate, 2) our photosensitivity to the florescence spectrum, and 3) the crystal's solid angle viewed by the detector. We find that standard UV grade CaF_2 is acceptable in our Long λ channel if its solid angle is limited by the slit, whereas the lower florescence-yield MgF_2 used in the Short λ can be placed close to the detector.

4. DETECTORS

The FUV spectrum from each channel is focused upon a microchannel plate (MCP) detector. Each channel has a separate Z stack of three 36 mm circular Photonis MCPs. The detectors employ an RbBr or CsI photocathode coating to improve sensitivity. High-quality QM MCPs are in-hand for development testing.

The plates are housed in a braised ceramic detector body which has a design closely derived from the detector body used in SOHO. The FM detector has been fabricated at UCB and is undergoing environmental tests.

The original SPEAR design concept used a single stack of large format rectangular plates. We found that problems of large format rectangular plates (deviations in QE over the surface of the stack, inability to arbitrarily rotate the pore angle to reduce moiré pattern noise and improve QE, and high cost) greatly outweighed the benefit of using a single stack. We have, however, maintained the use of a single anode for both fields of view. The single anode allows us to use a single set of detector electronics, conserving weight, power, and volume.

The SPEAR concept anode design used dual delay lines with charge division providing measurement along one axis, and delay measurement providing the second axis. During development it became apparent that differential non-linearity and fixed pattern noise in this design would limit the sensitivity of the instrument to diffuse emission. This prompted a change to a cross delay line anode system. The cross delay line anode uses delay timing for both axes. The axes of the anode are rotated 15 degrees with respect to the spectral and imaging axes of the optics. Any non-linearity in the anode or electronic will not mimic a spectral feature because of this rotation.

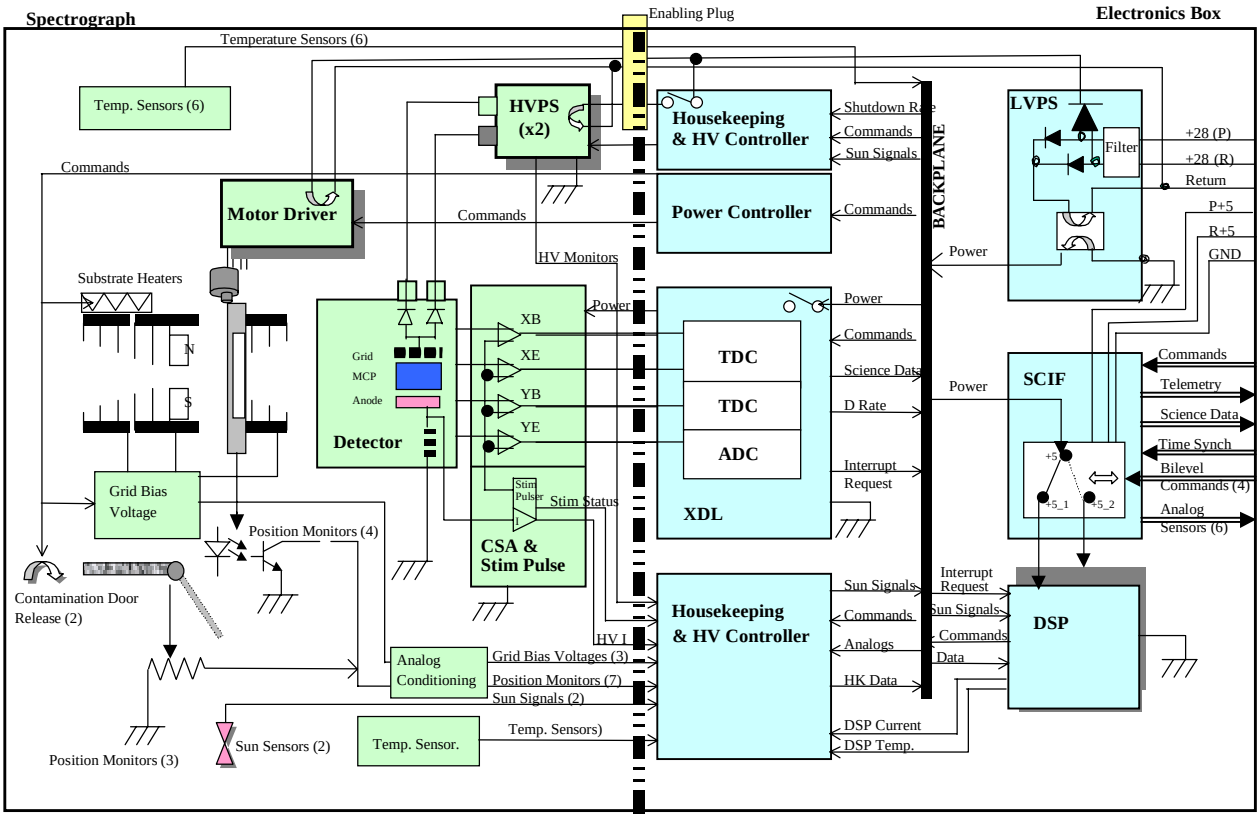

Figure 6: Instrument schematic

4.1 Detector Electronics

The detector anode output is amplified using dual two-channel high-speed amplifiers similar to the designs used in previous detector systems fabricated at UCB. The external delay line is fabricated on a PCB that is integrated into the Amp unit. This delay line is more compact than the coaxial cable delay used in some instruments. Each amplifier provides two high speed (5 ns FWHM) timing channels and a single bipolar 1 μs shaped output with peak voltage proportional to the input charge. A stimulation unit (STIM) injects an artificial event signal into the detector electronics front end at a fixed interval so that thermal drifts in the position encoding system can be calibrated in flight.

Each amplifier's differential timing output is digitized using a time-to-digital converter (TDC). This TDC is a dual stage system, with the first stage providing time-to-amplitude conversion followed by analog to digital conversion using an AD 679 ADC. The TDC system also includes an 8-bit ADC for digitizing the charge output of the amplifier system as a monitor of detector health. To improve noise isolation the X and Y TDC channels are handled on separate PC boards, each contained in their gold-over-nickel plated aluminum housing. See Fig. 6 for an electronics block diagram.

A programmable count rate monitor protects the detector system from damage at high count-rates by commanding high voltage to a low level when data rates exceed a commandable threshold. To avoid data loss in sky survey mode due to

stars transiting the field of view, the DSP software automatically recovers from rate shutdown mode. If two recovery attempts fail due to continued high count-rate, the shutdown state is maintained until commanded from the ground.

Detector high voltage is provided by dual-redundant diode-mixed Spacom -6 kV HV supplies. The HVPS are mounted directly to the detector back plate, eliminating the need for HV cables. More details of the detector and associated electronics can be found in Nam et al. [2002].

5. PAYLOAD CONTROL AND DATA HANDLING ELECTRONICS

5.1 Payload Control

The payload is controlled by the SPEAR instrument controller (SIC) that consists of dual redundant on-board DSP processor boards. These boards use the Lucent DSP32C 32 bit processor. The DSPs have been TID radiation tested and are latch-up protected. The board implements 512 Kbyte EDAC protected SRAM used as program storage, instrument health data storage, and science data storage. The board design is similar to the design of the EURD system and includes watchdog and latch-up protection. The EDAC design is derived from KITSAT-3 designs.

The active DSP is selected using discrete commands from the spacecraft that switch power to the DSP boards. Communications to the spacecraft node controller network (NC) are conducted over dual 9.6 kbps RS-422 serial lines. One of these lines is connected to the primary. The other is connected to the backup network. Either DSP can use either link. These links are used primarily for spacecraft commands to the instrument, command responses, and real-time state of health data.

Science and stored state-of-health data are transmitted to the dual mass memory subsystems (MMS) over 200 kbps one-way serial links. Again, each DSP can communicate with either MMS. Both the NC network and MMS serial links are implemented on a single SPEAR Spacecraft Interface (SCIF) PC board. Performing QM units of the SIC and the SCIF have been made and are in qualification testing. Should both MMS systems or both payload data transmitters fail, science data can be transmitted at low rate to the spacecraft on-board computer (OBC) over the NC Network. The SPEAR payload data memory has been sized to allow a minimum science mission of 90 minutes of astronomy observations per day in this contingency mode.

5.2 Power Distribution and Control

Power to instrument subsystems is provided by space qualified radiation hardened Interpoint SMTR series DC-DC converter modules. The instrument requires +5V (digital subsystems), ±5V (detector subsystems), ±12V (detector subsystems), and unregulated 28V (HV converters, Optics heaters, dust cover and shutter subsystems). The ±5V power is provided via linear regulators operating on the ±12V supplies. Dual redundant 28V input power to these modules is mixed using MOSFET switches.

Power to the instrument subsystems is switched by command of the DSP. Power to the shutter, HV converters, heaters, and dust covers is switched on a separate power control (CTRL) board using solid state opto-MOSFET switches. This board also controls cover activation and shutter motion. A Green-Tag Enable Plug allows HVPS and door activation in the flight configuration only.

The CTRL board contains redundant opto-isolated H-bridge circuit to drive the shutter stepping motor. Power to the detector electronics is switched using MOSFETs aboard the TDC subsystem. Extra care has been taken to isolate and filter digital and power system noise from sensitive analog power lines.

5.3 Housekeeping and HV Control

A housekeeping (HK) board provides monitors for critical instrument parameters including subsystem temperatures, LVPS input and output voltage levels, LVPS current draw, cover position, shutter position, HVPS output voltage, and

detector current draw. Monitors are selected using two 16 input analog multiplexors (MUX) and digitized using an 8 bit ADC. The HK board also includes digital-to-analog converters (DAC) to set HV supply output voltage.

6. SOFTWARE

The SPEAR flight software consists of 8500 lines of C code. A single main operations loop controls the operations of the instrument. (Fig 7) The main loop handles 1) packetization and flow control of science data, 2) control of the shutter motor, 3) command processing and response, 4) storage and transmission of housekeeping data, 5) time synchronization between payload and OBC, 6) detection and potential recovery from shutdown conditions and 7) management of transmission to the MMS via direct memory access (DMA).

Detector events (here after called "Photons") trigger a DSP interrupt. The interrupt service routine (ISR) transfers event data into a queue for later processing. In order to preserve photon timing information for later synchronization with spacecraft attitude data a 10 Hz timer also triggers events into this queue. These time events contain both the current payload time word and the state of the S/C 1 Hz clock, to allow easy synchronization with S/C time. The packetization and flow control routine transfers these events and stores them into packets for transmission to the MMS. The DMA manager manages the transmission of completed packets to the MMS.

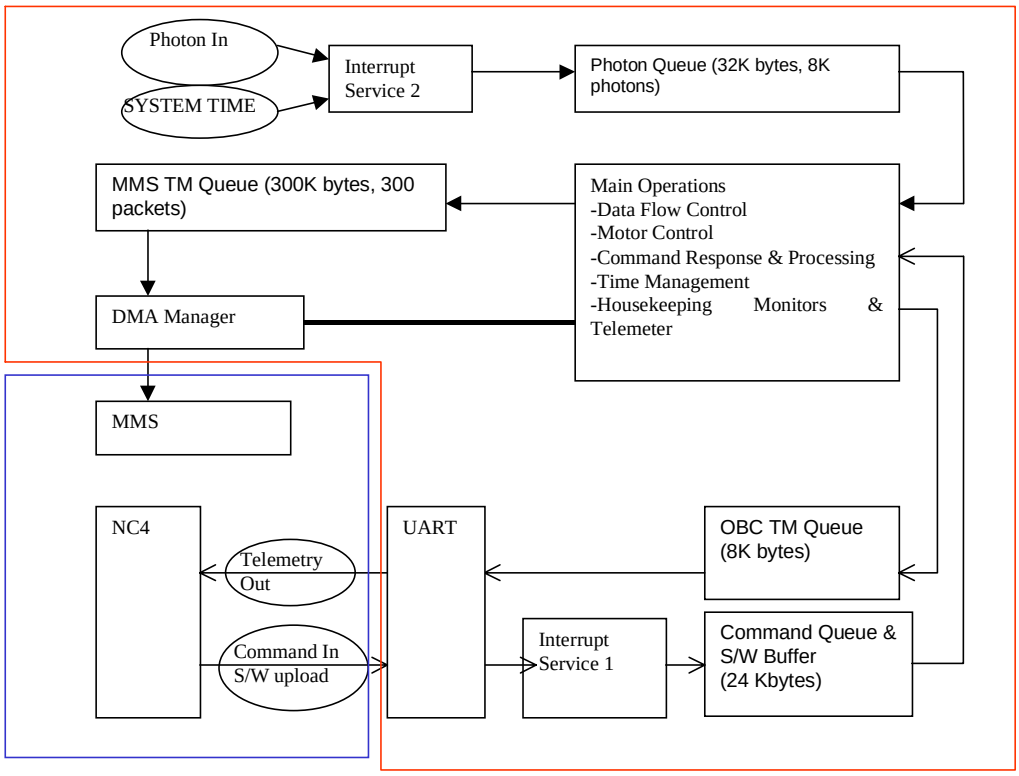

Figure 7: Flow Diagram of the Instrument Software

Command transmissions via the NC network are received via a second ISR. When a complete command packet has been received and verified, it is executed. Received commands are echoed to the data stream and verified before execution.

At set intervals (which can be modified by command) the DSP samples each housekeeping monitor. These monitors are both sent to the OBC via the NC network (for use as whole-orbit state-of-health data and for real time monitors during ground passes) and are stored into packets for transmission to the MMS within the science data.

Control of the shutter during observations is via tables stored in DSP RAM. This table contains step position and dwell time for each of the filter positions. The "Start Observing" command has a parameter that chooses from four possible tables. The contents of each of these tables can be changed during the mission via uplinked command. At each shutter motion a "shutter step record" is inserted into the photon data stream.

In order to recover sky position of detected photons, it is necessary to have time synchronization between the SPEAR payload and OBC attitude reports. The S/C real-time clock generates a 1 Hz clock that is provided to the SPEAR payload for time synchronization purposes. At the start and end of each observation, the SPEAR clock is synchronized with the OBC clock using a command. Upon request from SPEAR, the OBC reports the time of the next rising edge of the 1 Hz S/C clock. Using this, and the time reports in the photon data stream, it is possible to determine the arrival time of a photon relative to the OBC attitude report to << 0.2 sec. This corresponds to a positional uncertainty for photon events of 1.4'.

The DSP software also implements detection and recovery from shutdown conditions. The recovery algorithms are active by default and can be overridden by ground command. SPEAR has two possible shutdown conditions: sun shutdown and rate shutdown. Sun shutdown occurs when photodiodes aligned with the instrument aperture detect the sun within 30 degrees of the SPEAR field of view. Upon detection of the sun, HV to the detector is shut down without DSP intervention. Each time through the main loop, the status of the sun shutdown hardware flag is checked. If it is set, the DSP commands the shutter to the closed position. No automatic recovery from sun shutdown is attempted.

Counters implemented in the TDC boards detect rate shutdown conditions. If a programmable rate threshold is exceeded, the HV output is programmed to a safe level. After 2 seconds, (about the time for an object to transit the FOV during sky survey) the HV is reset to operational level. If a second shutdown occurs within 30 seconds, the delay to HV reset is increased to 5 seconds. If a third shutdown occurs within 30 seconds, no recovery is attempted, status is reported and the system awaits a ground command.

Operating software can be uploaded in part or whole. The code, resident in ROM, is RAM loaded at boot. If RAM load fails, or at the election of ground command, a ROM based uploader will be activated. Code is compiled in block boundaries with tags to facilitate modular upload modification of subroutines. Uploads can span several orbital contacts if required.

7. STATUS

As of late July, 2002, the bulk of SPEAR flight model components have been fabricated. The flight instrument is being assembled. Flight electronics are undergoing integrated testing. Flight mirrors are being coated at GSFC. Flight gratings are scheduled for delivery in the coming weeks.

8. ACKNOWLEDGEMENTS

This work was supported by NASA Space Astrophysics Research and Analysis grant NAG-5-5335. SPEAR instrument and KAISTSAT-4 development has been funded by the Korean Ministry of Science and Technology through the Korean Astronomy Observatory and the Korea Advanced Institute for Science and Technology.

REFERENCES

1. Bowyer, S., Korpela, E., Edelstein, J., Lampton, M., Morales, C., Perez-Mercader, J., Gómez, J. , & Trapero, J., "Evidence Against the Sciama Model of Radiative Decay of Massive Neutrinos," *ApJ*, **526**, 10, 1999.
2. Dixon, W.V., Sallmen, S., Hurwitz, M., & Lieu, R., "Far-Ultraviolet Spectroscopic Explorer Detection of Diffuse Galactic O VI Emission toward the Coma and Virgo Clusters," *ApJ*, **552**, 69L., 2001.
3. Edelstein, J., et al., "The SPEAR (Spectroscopy of Plasma Evolution from Astrophysical Radiation) Mission," *Proc. SPIE*, **4854** (this volume), 2002.
4. Edelstein, J., Bowyer, S., Korpela, E., Lampton, M., Trapero, J., Gómez, J.F., Morales, C., & Orozco, V., "EURD Observations of Interstellar Radiation," *Ap&SS*, **276**, 177, 2001.
5. Edelstein, J., Dixon, W.V., & Korpela, E., "Galmatheia: A Galactic Plasma Explorer," in *Ultraviolet - Optical Space Astronomy Beyond HST*, ed. Shull, Kinney and Morse, *ASP Conf Series*, **164**, 307, 1999.
6. López-Moreno, J., Morales, C., Gómez, J., Trapero, J., Bowyer, S., Edelstein, J., Korpela, E., & Lampton, M., "Spectrum of the Extreme Ultraviolet Nightglow as Measured by EURD," *Ap&SS*, **276**, 211, 2001.
7. Martin, C., & Bowyer, S., "Discovery of high-ionization far-ultraviolet line emission from the interstellar medium," *Asp*, **350**, 242, 1990.
8. McCammon, D., Almy, R., Apodaca, E., Bergmann, W., Deiker, S., Galeazzi, M., Lesser, A., Sanders, W., Figueroa, E., Kelley, R. L., Porter, F. S., Stahle, C. K., & Szymkowiak, A. E., "High Spectral Resolution Observations of the Soft X-ray Diffuse Background with Thermal Detectors". *B.A.A.S*, **195,** 135.04, 1999.
9. Nam, U.-W., et al., "Microchannel Plate Detector Electronics System for SPEAR," *Proc. SPIE*, **4854** (this volume), 2002.
10. Ryu, K.S., et al., "Optics Development for the SPEAR mission," *Proc. SPIE*, **4854** (this volume), 2002.
11. Ryu, K.S., Seon, K.I., Yuk, I.S., Seon, J.H., Nam, U.W., Lee, D.H., Min, K.W., Han, W., Edelstein, J., & Korpela, E.J., "Tolerance Analysis of FIMS Optical System," *JASS*, **17**, 67, 2000.
12. Seon, K.I., Ryu, K.S., Yuk, I.S., Park, J.H., Nam, U.W., Han, W., Seon, J.H., Min, K.-W., Edelstein, J., & Korpela, E.J., "OVI Emission Line Detection Limit of Far-Ultraviolet Imaging Spectrograph," *JASS*, **17**, 77, 2000.
13. Shelton, R.L., et al. "Observations of O VI Emission from the Diffuse Interstellar Medium," *ApJ*, **560,** 730, 2001.